Emergence of the interplay between hierarchy and contact splitting in biological adhesion highlighted through a hierarchical shear lag model

Lucas Brely[(1)], Federico Bosia[(1)], and Nicola M. Pugno[(2,3,4)*]

(1) Department of Physics and "Nanostructured Interfaces and Surfaces" Inter-Departmental Centre, Università di Torino, Via P. Giuria 1, 10125, Torino (Italy).

(2) Laboratory of Bio-Inspired & Graphene Nanomechanics, Department of Civil, Environmental and Mechanical Engineering, Università di Trento, via Mesiano, 77, I-38123 Trento, Italy.

(3) School of Engineering and Materials Science, Queen Mary University of London, Mile End Road, London E1 4NS.

(4) Ket Lab, Italian Space Agency, Via del Politecnico snc, 00133 Rome, Italy

(*) Corresponding author: *nicola.pugno@unitn.it*

Abstract

Contact unit size reduction is a widely studied mechanism to improve adhesion in natural fibrillar systems, such as those observed in beetles or geckos. However, these animals also display complex structural features in the way the contact is subdivided in a hierarchical manner. Here, we study the influence of hierarchical fibrillar architectures on the load distribution at the interface between the contact elements and the substrate, and the corresponding delamination behaviour. We present an analytical model to derive the load distribution in a fibrillar system, including hierarchical splitting of contacts, i.e. a "hierarchical shear-lag" model that generalizes the well-known shear-

lag model used in mechanics. The influence on the detachment process is investigated introducing a numerical procedure that allows the derivation of the maximum delamination force as a function of the considered geometry, including statistical variability of local adhesive energy. Our study suggests that contact splitting alone is insufficient to produce efficient adhesive performance, and needs to be coupled with hierarchical architectures to counterbalance high load concentrations resulting from contact unit size reduction, generating multiple delamination fronts and helping to avoid detrimental non-uniform load distributions. We show that these results can be summarized in a generalized adhesion scaling scheme for hierarchical structures, proving the beneficial effect of multiple hierarchical levels. The model can thus be used to predict the adhesive performance of hierarchical adhesive structures, as well as the mechanical behaviour of composite materials with hierarchical reinforcements.

Keywords: Biological adhesion, Bioinspired, Hierarchy, Delamination, Finite Element Model.

1. Introduction

Animal adhesive pads based on dry friction, such as those found in insects, spiders [1] [2] or geckos [3] share a common strategy to enable optimized attachment to a non-adhesive substrate: contact is achieved through a large number of fibrillar structures that interact with the surface through Van der Waal's interactions [4] and capillary forces [5]. It has been shown that the adhesive strength of the contact pads increases as the size of the terminal elements (i.e. spatulae or setae) decreases and their number increases [6]. Indeed, contact models such as that by Johnson, Kendall and Roberts (JKR) [7] predict an unlimited increase in the adhesive strength as the size of the contact tips decreases. This decrease in size also leads to an increase of the total peeling line, i.e. the sum of all contact tip widths, which is proportional to the peeling force according to thin-film peel theories [8]. Additionally, as the size of the animal increases and the dimensions of the contact units are reduced, hierarchical splitting is observed. For example in geckos, the lamellae support so-called setae, which are themselves split into hundreds of spatulae [3]. Similar structures are observed in arachnids [2]. The hierarchical scheme of contact splitting has been described as a way to optimize surface adaptability [9] or self-cleaning abilities [10] and to avoid self-bunching [11], and has been extended not only to the hairy adhesive structures, but also to the spider silk anchorages [12] [13] [14]. With the recent introduction of artificial micro-patterned surface that mimic animal adhesion [15] [16], including hierarchical structures [17] [18], reliable analytical/numerical approaches need to be developed in order to derive optimization criteria for such systems [19], and the interplay between contact size and hierarchical organization needs to be adequately addressed.

Energy balance is usually adopted to analytically describe the delamination of a tape from a substrate. Two main models are extensively cited in the study of adhesion: the Rivlin model [20],

which provides the peeling force, i.e. the tension required to achieve delamination in the detached length of an inextensible tape as a function of the adhesive energy, and the Kendall model [21], which includes the tape elastic energy variation in the equilibrium equation. Both models predict an increase in the peeling force as the angle between tape and substrate decrease. It has been shown that this relation correctly describes animal attachment systems [22] [23] [24] [25]. Geckos, for example, use opposing legs to stick to a surface in an inverted, upside-down position, thus reducing the peeling angle and optimizing adhesion. At the scale of microscopic contacts, reducing the peeling angle affects the distribution of load at the interface, which is another important aspect of the delamination mechanism. Indeed, interface stress is not uniform and depends on the structural and loading geometries. Models describing of the stress distribution as a function of the system geometrical and mechanical properties based on detailed experimental studies using pressure sensitive adhesive tapes were proposed in the 60's and 70's. One example is the Kaelble model [26], in which analysis of the interface stress has highlighted a direct relationship between the peeling angle and the critical stress in the adhesive layer. Stress distributions are obtained through the balance of forces acting on the tape in the attached region. When the applied external load is parallel to the substrate, the force balance can be reduced to a 1D problem, usually referred to as the "shear-lag model" [27], leading to a simple description of the load distribution. This loading configuration corresponds to the case in which the detachment force reaches its maximum, and is representative of the loading condition acting on biological contact elements (e.g. a gecko toe pad) in a stable attached configuration.

In this work, we propose an extension of a classical shear-lag model [27] to hierarchical configurations and introduce a numerical approach to simulate the detachment process of thin films with an arbitrary (including hierarchical) structure from rigid substrates, with the objective of

calculating the load distributions acting on their contact units, validating the theory and providing predictions for the peeling force of hierarchical adhesives or the pull-out force of hierarchical reinforcements in composites [28].

2. Hierarchical shear lag model

A schematic representation of a hierarchical attachment system is given in *Figure 1*. As explained above, we limit our study to the case of a load directed parallel to the substrate, since this provides significant insight in the role of hierarchy and contact splitting, starting from the analysis of the corresponding load distributions, and their influence on delamination. Rather than directly transferring the load between the tape (level-1 structure) and the interface, intermediate structures are introduced (level 2, level 3…) in the form of arrays of smaller tapes. The attachment system thus becomes a self-similar structure that transfers load through hierarchically organized contact units. The force acting on an infinitesimal length of the h-level tape is shown in *Figure 1*. At each scale level h, the tape geometrical and mechanical properties are the width w_h, the thickness b_h, the attached length L_{ah}, the displacement in the attached region u_h, the detached length L_{dh}, the elastic modulus E_h, the axial force within the tape F_h, and the number of sub-units N_h, i.e. the number of level-(h+1) structures attached to the h-level tape. The attachment contains $\prod_h N_h$ contact units in total.

We adopt a top-down strategy to determine the load supported by each contact, starting from the larger (level-1) structure. When the structure is constituted by two levels, the load transfer between level 1 and level 2 is obtained from the force balance on an infinitesimal length of the level-1 attached region $\mathrm{d}x_1$, as:

$$\frac{\mathrm{d}F_1}{\mathrm{d}x_1} = \frac{N_1}{L_{a1}} F_2 \tag{1}$$

where $\mathrm{d}F_1$ is the variation of axial load over $\mathrm{d}x_1$ and $N_1 \cdot \mathrm{d}x_1/L_{a1}$ is the number of contact units contained in the infinitesimal length $\mathrm{d}x_1$. The load transferred to level-2 is assumed to be constant over the width of the level-1 tape. The axial force in each contact is:

$$F_2 = \frac{E_2 b_2 w_2}{L_{d2}} u_1 \tag{2}$$

where u_1 is the axial displacement in the level-1 structure. Substituting Eq. (2) into Eq. (1) and writing the strain in the level-1 structure as $\epsilon_1 = \mathrm{d}u_1/\mathrm{d}x_1 = F_1/(E_1 b_1 w_1)$, we obtain after differentiation:

$$\frac{\mathrm{d}^2 F_1}{\mathrm{d}{x_1}^2} = \frac{N_1}{L_{a1}} \frac{E_2 b_2 w_2}{L_{d2} E_1 b_1 w_1} F_1 = \lambda_1 F_1 \tag{3}$$

We apply the boundary condition $F_1(x_1 = 0) = F_0$, where F_0 is the applied external load, and suppose that the length L_{a1} is sufficiently long for the axial load to tend to 0 at the other tape end (as is verified in all the cases considered in this study). This is equivalent to imposing

$F_1(x_1 = -\infty) = 0$. We obtain from Eq. (2) and Eq. (3) the load distribution on the first and second-level as:

$$F_1(x_1) = F_1(x_1 = 0)exp\left(\sqrt{\lambda_1}x_1\right) \tag{4}$$

Using Eq. (1) together with Eq. (4) we have:

$$F_2(x_1) = F_1(x_1 = 0)\frac{L_{a1}}{N_1}\sqrt{\lambda_1}exp\left(\sqrt{\lambda_1}x_1\right) \tag{5}$$

and repeating the procedure iteratively for the following levels, we obtain:

$$F_3(x_1, x_2) = F_2(x_1)\frac{L_{a2}}{N_2}\sqrt{\lambda_2}exp\left(\sqrt{\lambda_2}x_2\right) \tag{6}$$

...

$$F_h(x_1 \cdots, x_h) = F_{h-1}(x_1, \cdots, x_{h-1})\frac{L_{ah}}{N_h}\sqrt{\lambda_h}exp\left(\sqrt{\lambda_h}x_h\right)$$

These results are valid when the deformations within the attached regions of the level *h* structure are small with respect to the deformation of those at level *(h-1)*, which is a valid assumption in most cases. If the attached length is not sufficiently long for the axial load to naturally tend to zero, Eq. (3) can be solved by imposing a boundary condition of the form $F_1(x_1 = -L_{a1}) = 0$, which leads to an analogous exponential form for the load distribution. This case is not considered here for simplicity and because the condition $F_h(-L_{ah}) = 0$ corresponds to a maximum of detachment force for the considered structure, which is the case of interest.

Figure 2 shows the typical contact unit load distribution for two- and three-level structures whose geometrical and mechanical properties are reported in Table 1 and Table 2, respectively, and an applied external load F_0. In the two-level structure (*Figure 2.A*), the contact units adhere to the substrate and are directly attached to the tape. The exponential distribution of force transferred to

the contact units presents a maximum at the peeling line ($x_1 = 0$). In the case of a three-level structure (*Figure 2.B*), an intermediate level has been included, consisting of a set of lamellae or sub-tapes. The distribution presents multiple potential detachment fronts, where local force maxima for each of the intermediate structures are observed. The detachment behaviour of the first structure can easily be predicted, as the "crack front" theoretically propagates for a constant pulling force as a result of local detachment events in the area close to the peeling front, referred as "process zone" [23]. In the second case, the delamination events in the intermediate structures are simultaneous and several crack fronts will be involved in the detachment process. In both scenarios, the force at which the system detaches is likely to be influenced by the specific overall load distribution. Note that the integral under the curves should be multiplied by the number of contacts in the width of the tape to be equivalent to the external load.

The dissipated energy by a detaching hierarchical structure can be obtained by considering the energy balance during delamination [21], which provides the relationship between the various energy terms involved when the detachment occurs, and can be written as follows:

$$\frac{dW_h}{dA_h} - \frac{dU_{e,h}}{dA_h} = \frac{dU_{I,h}}{dA_h} \tag{7}$$

where W_h is the work of the external force during detachment, $U_{e,h}$ is the stored elastic energy in the adhesive, $U_{I,h}$ the available energy at the interface between the adhesive and the substrate and A_h the adhesive area at level h. The interface energy in a hierarchical system is the total energy that the lower scale structures can dissipate per unit area of contact before complete detachment, so that:

$$\frac{dU_{I,h-1}}{dA_{h-1}} = \frac{W_h}{A_h} \tag{8}$$

In the hierarchical scheme, the total amount of dissipated energy is therefore obtained as:

$$W_{h-1} = \int_{A_{h-1}} \frac{W_h}{A_h} dA_{h-1} + U_{e,h-1} \tag{9}$$

3. Numerical model

To verify the mechanisms outlined in the previous Section, we develop a numerical procedure to simulate the complete detachment of both types of structure. The system is discretized and modelled using a linear system of equations based on the Finite Element Method (FEM) in one dimension [29]. In particular, for a two-level system, the length $L_{a1}$is discretized in n_1 segments of length L_{a1}/n_1, each containing N/n_1 contacts. The linear system of load-displacement equations of size ${n_1}^2$ is written as $\mathbf{Q} = \mathbf{K}\,\mathbf{u_1}$, where $\mathbf{K}$ is the stiffness matrix that is derived using Eq. (2) and explicitly provided in the Appendix. The external load F_0 is applied on the terminal element of the discretized tape, so that the external force vector is $\mathbf{Q}(j) = F_0$ for $j = n_1$ and $\mathbf{Q}(\mathrm{j}) = 0$ for $j \neq n_1$. The equilibrium is written as $\mathbf{u_1} = \mathbf{K^{-1}Q}$ and the load distribution acting on each contact unit is then computed from the corresponding displacement field.

For a three-level structure, the length L_{a2} is discretized in $(n_2 - 1)$ segments of length $L_{a2}/(n_2 - 1)$ each of which contains $N_2/(n_2 - 1)$ sub-units, and we add one detached segment of length L_{d2}, resulting in a linear system of size $(n_1 n_2)^2$. The number of levels can be increased following the same iterative procedure. The explicit form of the stiffness matrix in this case is also provided in the Appendix.

Simulations are performed by imposing a stepwise incremental displacement. To introduce delamination in the model, a force threshold is assigned to each contact unit, above which the

contribution of the corresponding element is removed from the linear system. The detachment force criterion is based on the thin film energy balance [21] applied to the loaded contact fibril, i.e. delamination occurs for

$$F_{h_C}(x_{h-1}) = \sqrt{2E_h b_h {w_h}^2 G} \tag{10}$$

where F_{h_C} is the detachment load of a single contact at level h and G the local adhesive energy per unit area between the tape and the substrate. In the numerical model, the elastic energy of a single contact is fully dissipated (complete detachment) as soon as the detachment force is reached, so that the total energy dissipated by the contact after loading is:

$$W_h = L_{d,h} w_h G \tag{11}$$

4. Results and discussion

4.1 Two-level (beetle-like) structures

In order to verify the role of fibrillar contact number and size in adhesion, simulations are performed with varying lengths and numbers of contact units. We consider a level-1 (non-hierarchical) structure, with fixed geometry and mechanical properties, and a level-2 structure with the same mechanical properties, both initially in contact with the substrate. The reference structure has the following properties: $N_1 = 10^4$, L_{a1} = 10 mm, w_1 = 1 mm, b_1 = 0.1 mm, $E_1 = E_2$ = 1 GPa, L_{d2} = 0.1 mm, w_2 = 0.01 mm and b_2 = 0.01 mm.

To evaluate the influence of the contact unit size, a η-fold reduction of the size is considered, allowing an increase in the total number of contacts to $N'_1 = N_1 \cdot \eta^2$, and a reduction in dimensions

to $L'_{d2} = L_{d2}/\eta$, $w'_2 = w_2/\eta$ and $b'_2 = b_2/\eta$. As a first approximation, the average adhesive energy increase with the reduction of the contact tip size predicted by contact models [7] is neglected. The resulting external force F_0 vs. displacement δ at the load application point is shown in *Figure 3.A* for different η values. In all cases, there is an initial linear elastic deformation phase, then the load reaches a plateau corresponding to the detachment phase. Combining Eq.(5) with Eq. (10), we obtain the theoretical force at which detachment initiates as:

$$F_{0_D} = \frac{N_1}{L_{a1}}\sqrt{\frac{2E_2 b_2 {w_2}^2 G}{\lambda_1}} = \sqrt{2\frac{N_1}{L_{a1}} L_{d2} E_1 b_1 w_1 w_2 G} \qquad (12)$$

Therefore, the overall (level-1) structure is bonded to the substrate trough an interface (level 2) that can dissipate an energy $N_1 W_2/L_{a1}$ per unit detached length, where W_2 is given by (11). Applying energy balance in Eq. (7) to this system leads to:

$$\frac{{F_{0_C}}^2}{2E_1 b_1 w_1} = \frac{N_1}{L_{a1}} L_{d2} w_2 G \qquad (13)$$

Thus, comparing Eq. (12) to Eq. (13), in this case $F_{0_D} = F_{0_C}$, which means that the global detachment force is reached as soon as the local detachment initiates.

Statistical distributions are also introduced in the numerical model for the adhesive energy *G* to capture the influence of surface defects and inhomogeneities, as occurs in real systems. Surface energies $G(x_h)$ are thus randomly assigned for each segment along x_h extracting the values from a Weibull distribution [30] with scale parameter $\gamma = 0.01$ MPa.mm and various shape parameters m. Despite statistical variation in the local detachment forces, the average global adhesive force generated by the system is relatively constant, and coincides with the theoretical value given in Eq. (12) taking the scale parameter of the distribution equal to γ (shown in the inset of *Figure 3.A)*. The adhesive strength σ_C of the level-2 structure can be written as:

$$\sigma_C = \frac{F_{2_C}}{b_2 w_2} \tag{14}$$

so that from Eq. (10) we obtain:

$$\sigma_C = \sqrt{\frac{2GE_2}{b_2}} \tag{15}$$

Thus, an η-fold reduction of the contact size ($b_2 \rightarrow b_2/\eta$) leads to an increase in the adhesive strength by a factor of $\sqrt{\eta}$, in accordance with results in [23]. This is due to the increase of the total peeling line, i.e. the sum of the width of the contact elements as their number increases, usually indicated by peeling theories as one of the main parameters governing adhesion [8]. On the other hand, the variation in the load distribution shown in *Figure 3.B* counteracts this positive effect, since the load is distributed over a smaller fraction of the available contacts as their size decreases, so that there is no dependence of the overall detachment force with η. Only a uniformly distributed load involving more contact units would generate a higher detachment force. Alternatively, to obtain an improvement in the delamination load with contact size reduction ($F_{0_C} \propto \sqrt{\eta},$), the latter should not be applied to the detached length of the contacts L_{d2} , although this might lead to increased self-bunching effects. From Eq. (9) and Eq. (11), the total dissipated energy W by this tape becomes:

$$W_1 = N_1 L_{d2} w_2 G + L_{a1} \frac{{F_{0_C}}^2}{2E_2 b_2 w_2} = G(N_1 L_{d2} w_2 + L_{a1} w_1) \tag{16}$$

According to this equation, the total dissipated energy is not influenced by η in this case, as verified in simulations in *Figure 3.A.*

4.2 Three-level (gecko-like) structures

We now introduce an additional intermediate structure, as discussed above in the load distribution analysis (*Figure 2*). The detachment force of the resulting 3-level structure is compared to the previous 2-level structure in *Figure 4.A.* The adhesive energy is assigned as in the previous simulation. Results show an improvement in the total detachment force for the 3-level structure, together with a net increase in the total dissipated energy (the integral of the force vs. displacement curve). Thus, hierarchical organization leads to a wider distribution of the contact load, and reduces the stress concentrations close to the peeling line. As previously, an analytical force at which detachment initiates can be calculated from Eqs. (4-7) as follows:

$$F_{0_D} = \frac{N_1 N_2}{L_{a1} L_{a2}} \sqrt{\frac{2 E_3 b_3 {w_3}^2 G}{\lambda_1 \lambda_2}} \tag{17}$$

Figure 4.B shows that the force plateau reached by the 3-level system is higher and longer compared to the force obtained from Eq. (17). This can be explained by the fact that the detachment process involves the creation of multiple "crack fronts", as illustrated in *Figure 4.B,* which is beneficial to the overall adhesive performance. The analytical force obtained from Eq.(17) provides the force at which the delamination process initiates, which is smaller than the maximal detachment force in this case. As the system starts to detach, an equilibrium between the propagation of different crack fronts is reached. A close-up of the load vs. displacement curve corresponding to detachment events in the early stage of the simulation is shown in the inset of *Figure 4.A,* with markers plotted when single contact unit detachments occur. To analytically

determine the force plateau in the hierarchical structure, we adopt a bottom-up analysis of the system. Each level-2 tape has a detachment force F_{0_C} (given by Eq. (12)). As for Eq. (16), we calculate the total energy dissipated by the isolated tape, leading to:

$$W_1 = N_2 L_{d3} w_3 G + (L_{a2} + L_{d2}) \frac{{F_{1_C}}^2}{2E_2 b_2 w_2} \tag{18}$$

From (7) we obtain the following relation between the stored elastic energy in the level-1 tape and the energy dissipated by the interfaces of the sub-levels:

$$\frac{{F_{0_C}}^2}{2E_1 b_1 w_1} = \frac{N_1 W_1}{L_{a1}} \tag{19}$$

which leads to:

$$F_{0_C} = \sqrt{2 \frac{N_1}{L_{a1}} E_1 b_1 w_1 W_1} \tag{20}$$

This load level is also plotted in. *Figure 4.A* , showing good agreement with numerical simulations. This indicates that the maximum load that an adhesive structure can bear is related more to the energy that can be dissipated by its interfacial contacts rather than to their delamination strength. Also, these results highlight the fact that as the contact sizes become critical, biological adhesives adopt hierarchical organization to maintain the presence of multiple peeling fronts over the whole length of the attached system, giving rise to optimized distributions and developing a maximal delamination force from a given overall contact area.

5. Thin-film hierarchical scaling laws

Generalizing the equations in Section 2 using Kendall's theory [21] to the detachment of a thin film at a peeling angle θ, the relationship between the available interface energy and the detachment force at a given level *h* is:

$$F_{h-1_c}(1-\cos\theta)+\frac{{F_{h-1_c}}^2}{2E_{h-1}b_{h-1}w_{h-1}}=w_{h-1}\frac{W_h}{A_h} \tag{21}$$

Assuming that the loading angle remains constant for all the structures involved, Eq. (9) gives:

$$\frac{W_{h-1}}{A_{h-1}}=l_{a,h-1}\frac{W_h}{A_h}+\left(l_{a,h-1}+l_{d,h-1}\right)\frac{{F_{h-1_c}}^2}{2E_{h-1}b_{h-1}w_{h-1}} \tag{22}$$

For a self-similar (fractal-like) thin film structure at $\theta=0$, i.e. the previously considered particular case of hierarchical shear lag, Eq. (22) becomes:

$$F_{h-1_c}=\sqrt{2E_{h-1}b_{h-1}{w_{h-1}}^2\frac{W_h}{A_h}} \tag{23}$$

The scaling of the dissipated energy between levels thus becomes:

$$\frac{W_{h-1}}{A_{h-1}}=\frac{W_h}{A_h}\left(2+\frac{l_{d,h}}{l_{a,h}}\right) \tag{24}$$

so that each additional level gives an increase in the adhesive strength of a factor of $\sqrt{2+\beta}$, where $\beta=\frac{l_{d,h}}{l_{a,h}}$ is the ratio between the detached and attached length of the tape units. To provide a practical example, we consider contacts in a tape-like geometry with the dimensions $w=l_a=10=b=l_d/10$. We assemble these contact units into a structure with a contact area 10^6 times larger and the same mechanical properties, introducing various possible hierarchical arrangements: two levels with a scale factor of 10^6 between them (1.000.000:1), b) three levels with a scale factor

of 10^3 between each of them (1000: 1000:1), and c) four levels with a scale factor of 10^2 between each of them (100:100:100:1). Of course, the scale factor should be a relatively large number since the proposed model implies that there is a scale change between two levels. *Figure 5.A* illustrates the scaling of global adhesive strength $F_{0_C}/(w_1 L_{a1})$ as a function of the hierarchical organization and the peeling angle. A clear advantage of multiple hierarchical levels is highlighted in terms of global detachment strength. The angle dependency is that known from single-peeling theory, but also appears to be affected by hierarchical organisations, as shown in *Figure 5.B.* This result is limited to small θ values since local variations of the peeling angle may occur otherwise.

6. Conclusions

In conclusion, we have developed a generalization of the shear lag model to describe hierarchical fibrillar systems such as those observed in gecko and arachnid attachments and applied it in numerical simulations. We have shown that improved adhesion in fibrillar structures is not simply due to contact splitting alone, but rather to hierarchical organization, giving rise to optimized load distributions, enabling reduced stress concentrations, and therefore a reduced risk of detachment. Also, hierarchical architectures provide the means to provide multiple delamination fronts once detachment initiates, and therefore to continue avoiding critical stress concentrations. Finally, the general scaling behaviour of the adhesion of hierarchical structures is discussed, showing a clear advantage in providing multiple hierarchical levels. Thus, the presented model and numerical procedure contribute to providing a better understanding of the mechanisms of adhesion of hierarchical structures and can be used to provide design and optimization criteria for artificial adhesive structures, as well as for optimized composite materials with hierarchical reinforcements.

Acknowledgements

N.M.P. is supported by the European Research Council PoC 2015 "Silkene" No. 693670, by the European Commission H2020 under the Graphene Flagship Core 1 No. 696656 (WP14 "Polymer Nanocomposites") and FET Proactive "Neurofibres" grant No. 732344. F.B. is supported by H2020 FET Proactive "Neurofibres" grant No. 732344. This work was carried out within the COST Action CA15216 “European Network of Bioadhesion Expertise: Fundamental Knowledge to Inspire Advanced Bonding Technologies”.

References

[1] S. Gorb, “Biological attachment devices: exploring nature's diversity for biomimetics.,” *Philosophical Transactions of the Royal Society of London A: Mathematical, Physical and Engineering Sciences,* vol. 366, no. 1870, pp. 1557-1574, 2008.

[2] S. Gorb, “Attachment devices of insect cuticle,” *Springer Science & Business Media,* 2001.

[3] Autumn, K.; Peattie, AM., “Mechanisms of adhesion in geckos,” *Integrative and Comparative Biology,* vol. 42, no. 6, pp. 1081-1090, 2002.

[4] Autumn, K.; Sitti, M.; Liang, Y.A. ; Peattie, A.M. ; Hansen, W.R. ; Sponberg, S.; Kenny, T.W.; Fearing, R.; Israelachvili, J.N.; Full, R.J.. , “Evidence for van der Waals adhesion in gecko setae,” *Proceedings of the National Academy of Sciences of the United States of America,* vol. 99, no. 19, pp. 12252-12256, 2002.

[5] Federle, W.; Riehle, M.; Curtis, AS; Full, RJ., “An integrative study of insect adhesion: mechanics and wet adhesion of pretarsal pads in ants,” *Integrative and Comparative Biology,* vol. 42, no. 6, pp. 1100-1106, 2002.

[6] E. Arzt, S. Gorb and R. Spolenak, “From micro to nano contacts in biological attachment devices,” *Proceedings of the National Academy of Sciences of the United States of America,* vol. 100, no. 19, pp. 10603-10606, 2003.

[7] Johnson, K. L.; Kendall, K.; Roberts, A. D. , “Surface energy and the contact of elastic solids,” *Proceedings of the Royal Society of London A: Mathematical, Physical and Engineering Sciences,* vol. 324, no. 1558, 1971.

[8] Varenberg, M.; Pugno, N.M.; Gorb, S.N. , “Spatulate structures in biological fibrillar adhesion,” *Soft Matter,* vol. 6, no. 14, pp. 3269-3272, 2010.

[9] Kim, T.W.; Bhushan, B., “Adhesion analysis of multi-level hierarchical attachment system contacting with a rough surface,” *Journal of Adhesion Science and Technology,* vol. 21, no. 1, pp. 1-20, 2007.

[10] Hansen, W. R.; Autumn, K., “Evidence for self-cleaning in gecko setae,” *Proceedings of the National Academy of Sciences of the United States of America,* vol. 102, no. 2, pp. 385-389, 2005.

[11] Yao, H.; Gao, H., “Mechanics of robust and releasable adhesion in biology: Bottom–up designed hierarchical structures of gecko,” *Journal of the Mechanics and Physics of Solids,* vol. 54, no. 6, pp. 1120-1146, 2006.

[12] Grawe, I.; Wolff, J.O.; Gorb., SN., “Composition and substrate-dependent strength of the silken attachment discs in spiders.,” *Journal of The Royal Society Interface,* vol. 11, no. 98, 2014.

[13] Wolff, JO; Grawe, I; Wirth, M; Karstedt, A; Gorb SN., “Spider's super-glue: thread anchors are composite adhesives with synergistic hierarchical organization.,” *Soft matter,* vol. 11, no. 12, pp. 2394-2403, 2015.

[14] Meyer, A.; Pugno, NM.; Cranford, SW., “Compliant threads maximize spider silk connection strength and toughness.,” *Journal of The Royal Society Interface,* vol. 11, no. 98, 2014.

[15] Kamperman, M., Kroner, E., del Campo, A., McMeeking, R. M. and Arzt, E., “Functional adhesive surfaces with “gecko” effect: The concept of contact splitting.,” *Advanced Engineering Materials,* vol. 12, no. 5, pp. 335-348, 2010.

[16] Del Campo, A.; Greiner, C.; Arzt, E.., “Contact shape controls adhesion of bioinspired fibrillar surfaces.,” *Langmuir,* vol. 23, no. 20, pp. 10235-10243, 2007.

[17] D. Brodoceanu, C. .. Bauer, E. Kroner, E. Arzt and T. Kraus, “Hierarchical bioinspired adhesive surfaces—a review,” *Bioinspiration & Biomimetics,* vol. 11, no. 5, 2016.

[18] Röhrig, M., Thiel, M., Worgull, M. and Hölscher, H. , “3D Direct Laser Writing of Nano-and Microstructured Hierarchical Gecko-Mimicking Surfaces.,” *Small,* vol. 8, no. 19, pp. 3009-3015, 2012.

[19] Bosia, F., Colella, S., Mattoli, V., Mazzolai, B., & Pugno, N. M., “Hierarchical multiple peeling simulations.,” *RSC Advances,* vol. 4, no. 48, pp. 25447-25452, 2014.

[20] R. S. Rivlin, “The effective work of adhesion,” *Paint Technology,* vol. IX, no. 106, p. 2611—2614, 1944.

[21] K. Kendall, “Thin-film peeling-the elastic term,” *Journal of Physics D: Applied Physics,* vol. 8, no. 13, p. 1449, 1975.

[22] Autumn, K.; Dittmore, A.; Santos, D.;Spenko, M.; Cutkosky, M. , “Frictional adhesion: a new angle on gecko attachment,” *Journal of Experimental Biology,* vol. 209, no. 18, pp. 3569-3579, 2006.

[23] N. Pugno, “The theory of multiple peeling,” *International journal of fracture,* vol. 171, no. 2, pp. 185-193, 2011.

[24] Brely, L.; Bosia, F.; Pugno, NM., “Numerical implementation of multiple peeling theory and its application to spider web anchorages.,” *Interface focus,* vol. 5, no. 1, 2015.

[25] Afferrante, L., Carbone, G., Demelio, G., & Pugno, N., “Adhesion of elastic thin films: double peeling of tapes versus axisymmetric peeling of membranes.,” *Tribology Letters,* vol. 52, no. 3, pp. 439-447, 2013.

[26] D. H. Kaelble, “Theory and analysis of peel adhesion: bond stresses and distributions,” *Transactions of The Society of Rheology,* vol. 4, no. 1, pp. 45-73, 1960.

[27] H. L. Cox, “The elasticity and strength of paper and other fibrous materials,” *British journal of applied physics,* vol. 3, no. 3, p. 72, 1952.

[28] H. Qian, E. Greenhalgh, M. P. Shaffer and A. Bismarck, “Carbon nanotube-based hierarchical composites: a review,” *Journal of Materials Chemistry,* vol. 20, pp. 4751-4762, 2010.

[29] Tirupathi, R.C.; Belegundu, A.D., Introduction to finite elements in engineering, Pearson, 2002.

[30] W. Weibull, “Ingenioersvetenskapsakad,” *Handlingar,* vol. 151, 1939.

Figures

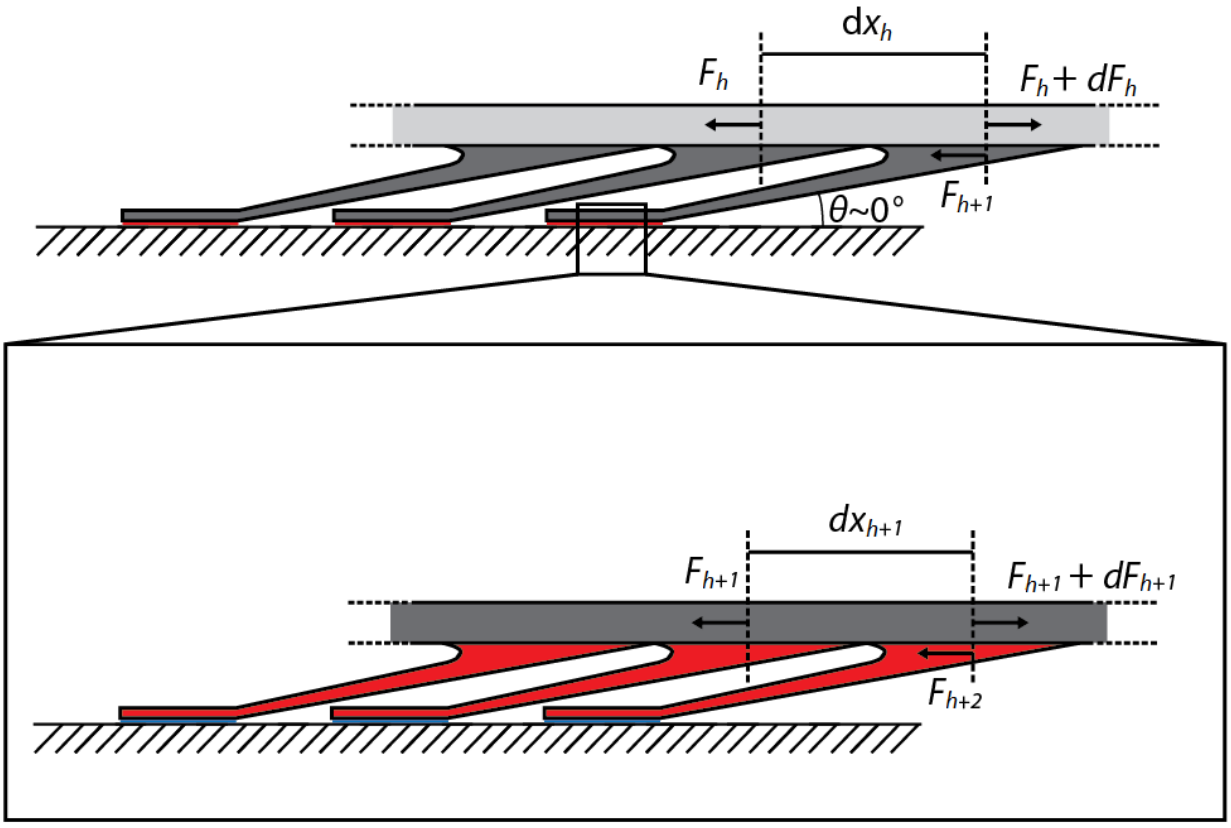

Figure 1 : Schematic representation of the hierarchical attachment system and the force equilibrium acting between two levels.

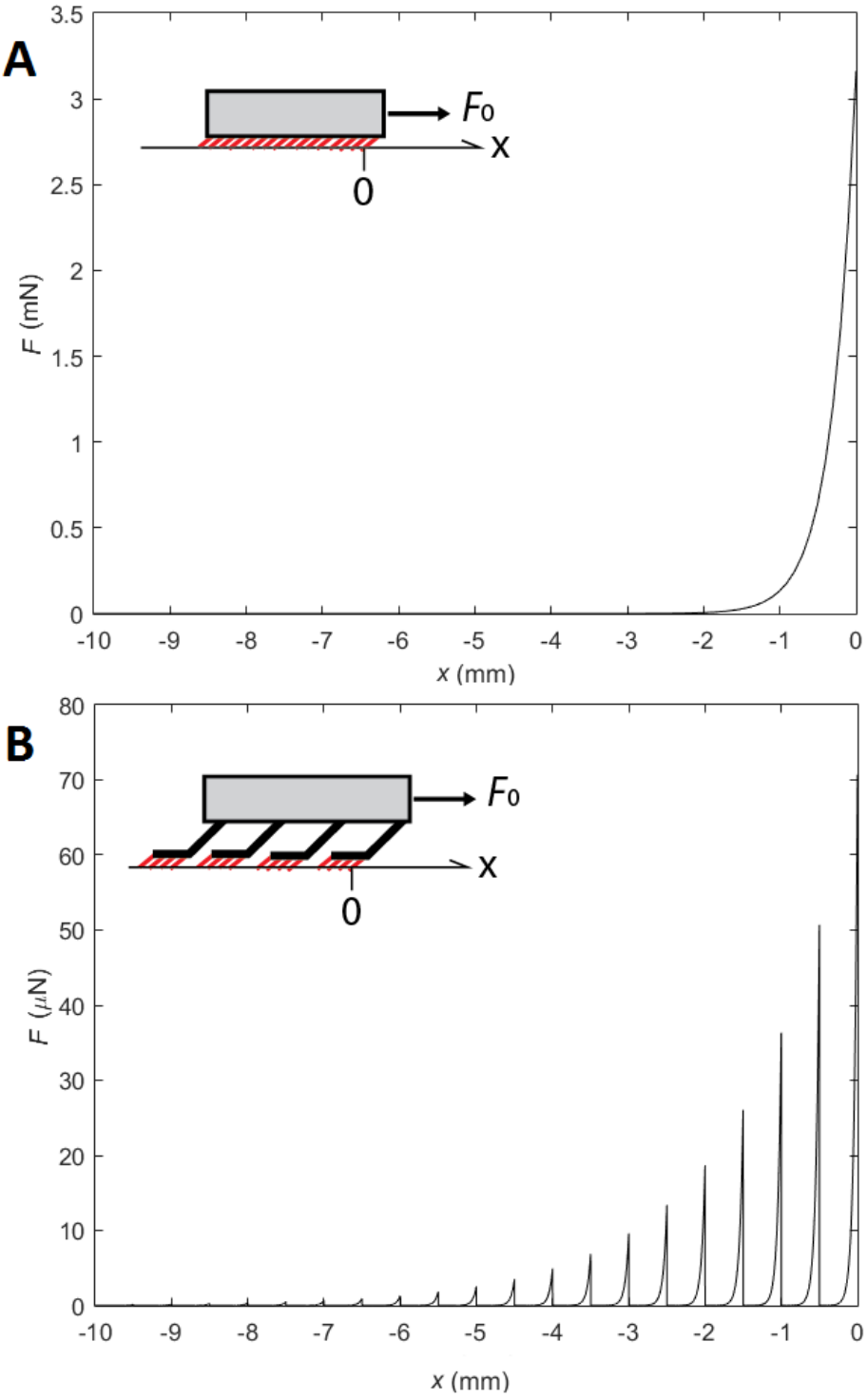

Figure 2 : Adhesion force distribution for 2-level (A) and 3-level (B) structures.

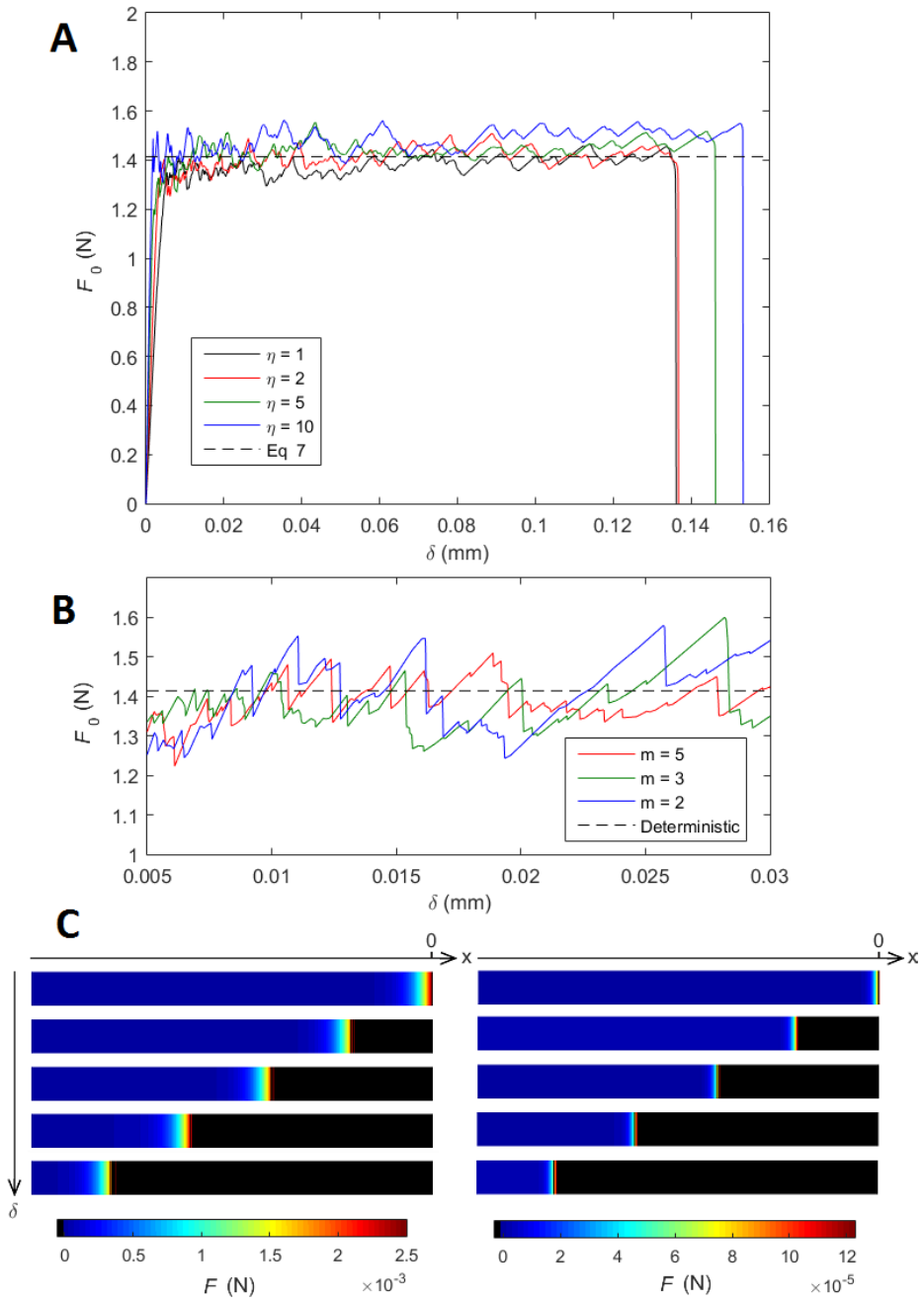

Figure 3: A. Force vs. displacement plots during detachment for different size reduction factors η. B. Force plateau for various shape parameter values of the Weibull distribution C. Propagation of the peeling front during delamination for $\eta = 1$ (left) and $\eta = 10$ (right). The color scale represents the contact unit force distributions. The area where contact units are detached is displayed in black.

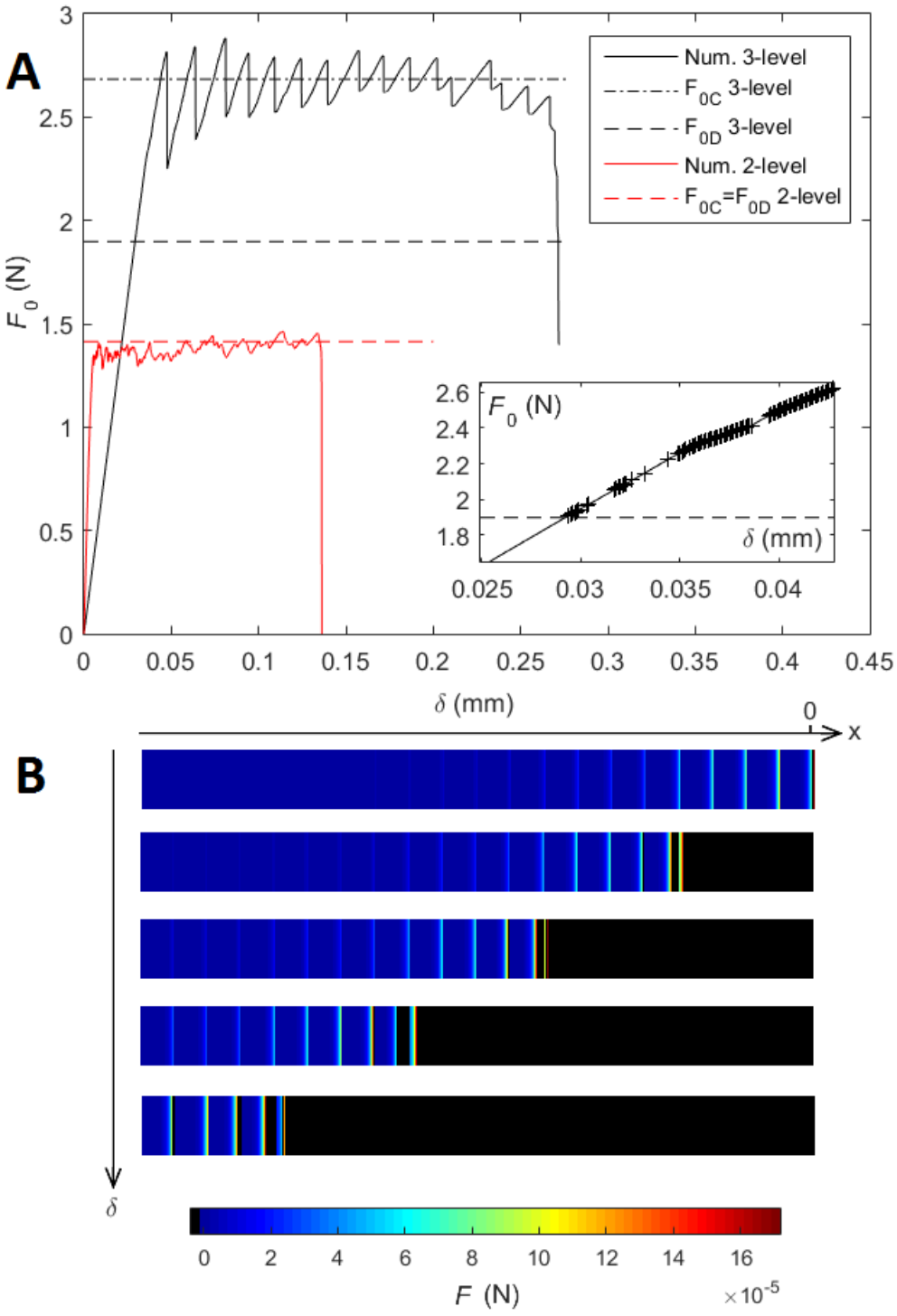

Figure 4 : A. Force vs. displacement curves for 2-level and 3-level structures. B. Propagation of the peeling front during simulation of the 3-level structures.

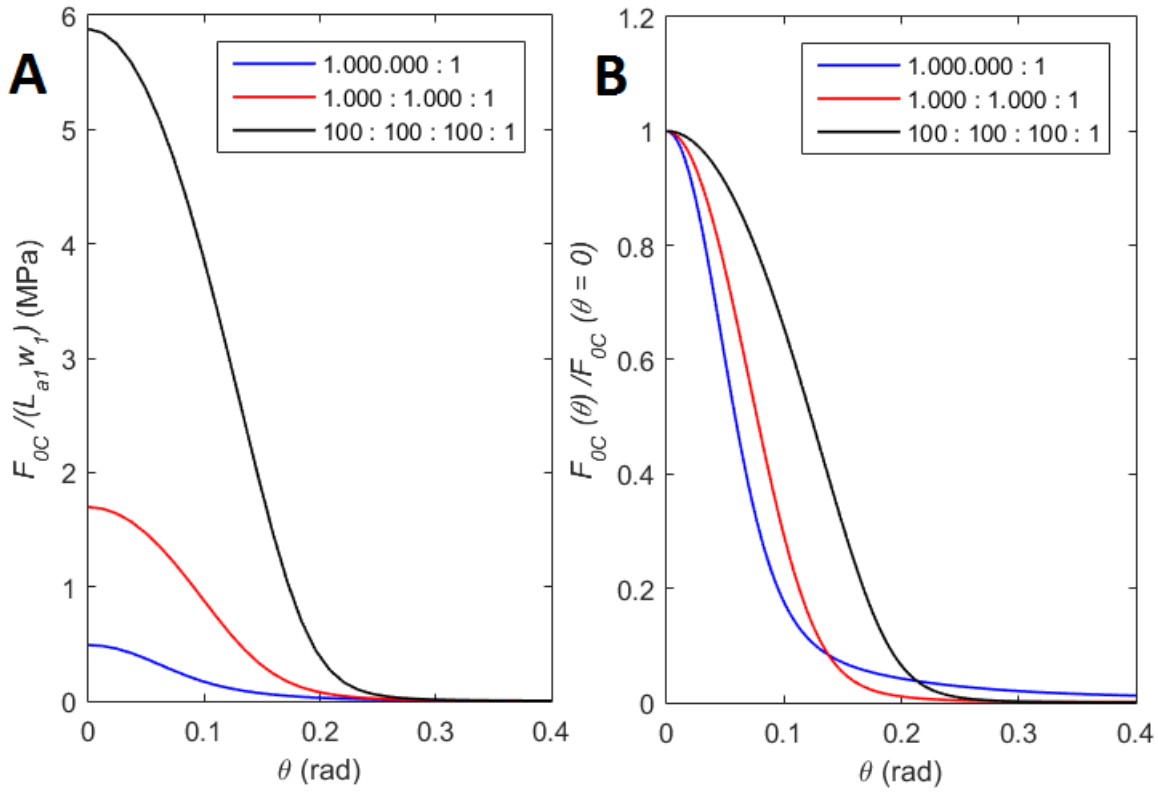

Figure 5 : Scaling of the adhesive strength of hierarchical self-similar tape structures: A) Overall adhesive strength as a function of peeling angle for 2-level (1.000.000:1), 3-level (1.000:1.000:1) and 4-level (100:100:100:1) structures with constant overall number of contacts. B) Overall adhesion force vs. peeling angle θ for the 3 structures, normalized with respect to the $\theta = 0$ value.

Tables

Level	E (MPa)	w (mm)	b (mm)	L_a (mm)	L_d (mm)	N
1	1000	1	0.1	10	-	10 000
2	1000	0.01	0.01	-	0.1	-

Table 1 : 2-Level structure geometrical and mechanical parameters.

Level	E (MPa)	w (mm)	b (mm)	L_a (mm)	L_d (mm)	N
1	1000	1	0.1	10	-	20
2	1000	1	0.02	0.5	1	50 000
3	1000	0.001	0.001	-	0.01	-

Table 2 : 3-Level structure geometrical and mechanical parameters.

Appendix

A Equations for the numerical model

For a two-level structure, the linear system of equations for the FEM simulations is banded and of size $n_1{}^2$:

$$\mathbf{K} = \begin{bmatrix} k_{a1}+k_{d2} & -k_{a1} & 0 & \cdots & 0 \\ -k_{a1} & 2k_{a1}+k_{d2} & \ddots & \ddots & \vdots \\ 0 & \ddots & \ddots & \ddots & 0 \\ \vdots & \ddots & \ddots & 2k_{a1}+k_{d2} & -k_{a1} \\ 0 & \cdots & 0 & -k_{a1} & k_{a1}+k_{d2} \end{bmatrix} \tag{A.1}$$

where $k_{a1} = n_1 E_1 b_1 w_1 / L_{a1}$ and $k_{d2} = N_1 E_2 b_2 w_2 / n_1 L_{d2}$, which we write as:

$$\mathbf{K} = \mathbf{K_{a1}} + \mathbf{K_{d2}} \tag{A.2}$$

where

$$K_{a1\,ij} = \begin{cases} k_{a1} \text{ for } (i=j=1) \cup (i=j=n_1) \\ 2k_{a1} \text{ for } (i=j) \cap (i \neq 1) \cap (i \neq n_1) \\ -k_{a1} \text{ for } (i = j \pm 1) \end{cases} \tag{A.3}$$

and

$$K_{d2\,ij} = k_{d2} \text{ for } (i = j) \tag{A.4}$$

For a three-level structure, the stiffness matrix is built as follows:

$$\mathbf{K} = \mathbf{K_{a1}} + \mathbf{K_{d2}} + \mathbf{K_{a2}} + \mathbf{K_{d3}} \tag{A.5}$$

where:

$$K_{a1\,ij} = \begin{cases} k_{a1}\ for\ \ (i = j = 1) \cup (i = j = n_1 n_2) \\ 2k_{a1}\ for\ \ (i = j = pn_2) \cap (i \neq n_2) \cap (i \neq n_1 n_2) \\ -k_{a1}\ \ for\ \ (i = pn_2) \cap (i = j \pm pn_2) \end{cases} \quad p \in \mathbb{N} \tag{A.6}$$

$$K_{d2\,ij} = \begin{cases} k_{d2}\ for\ \ (i = j = pn_2) \cup (i = j = pn_2 - 1) \\ -k_{d2}\ for\ (i = j + 1) \cap (i = pn_2) \\ -k_{d2}\ for\ (i = j - 1) \cap (j = pn_2) \end{cases} \quad p \in \mathbb{N} \tag{A.7}$$

$$K_{a2\,ij} = \begin{cases} k_{a2}\ for\ \ (i = j = 1) \cup (i = j = pn_2 \pm 1) \\ 2k_{a2}\ for\ (i = j) \cap (i \neq 1) \cap (i \neq pn_2) \cap (i \neq pn_2 \pm 1) \\ -k_{a2}\ \ for\ \ (i = j - 1) \cap (i \neq pn_2) \cap (i \neq pn_2 - 1) \\ -k_{a2}\ \ for\ \ (i = j + 1) \cap (j \neq pn_2) \cap (j \neq pn_2 + 1) \end{cases} \quad p \in \mathbb{N} \tag{A.8}$$

$$K_{d3\,ij} = k_{d3}\ for\ (i = j) \cap (i \neq pn_2)\ \ p \in \mathbb{N} \tag{A.9}$$

and $k_{a1} = n_1 E_1 b_1 w_1 / L_{a1}$, $k_{d2} = N_1 E_2 b_2 w_2 / (n_1 L_{d2})$, $k_{a2} = n_2 E_2 b_2 w_2 / L_{a2}$ and $k_{d3} = N_2 E_3 b_3 w_3 / ((n_2 - 1) L_{d3})$.

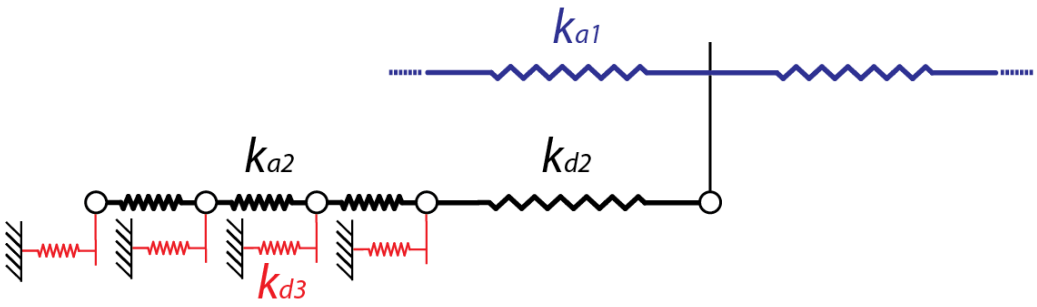

Figure A.1 Schematization of the hierarchical connectivity of elements (corresponding to the above stiffness matrix) used in the simulations.